Cell Reports
Physical Science

CellPress
OPEN ACCESS

Article

Applying the intrinsic principle of cell collectives to program robot swarms

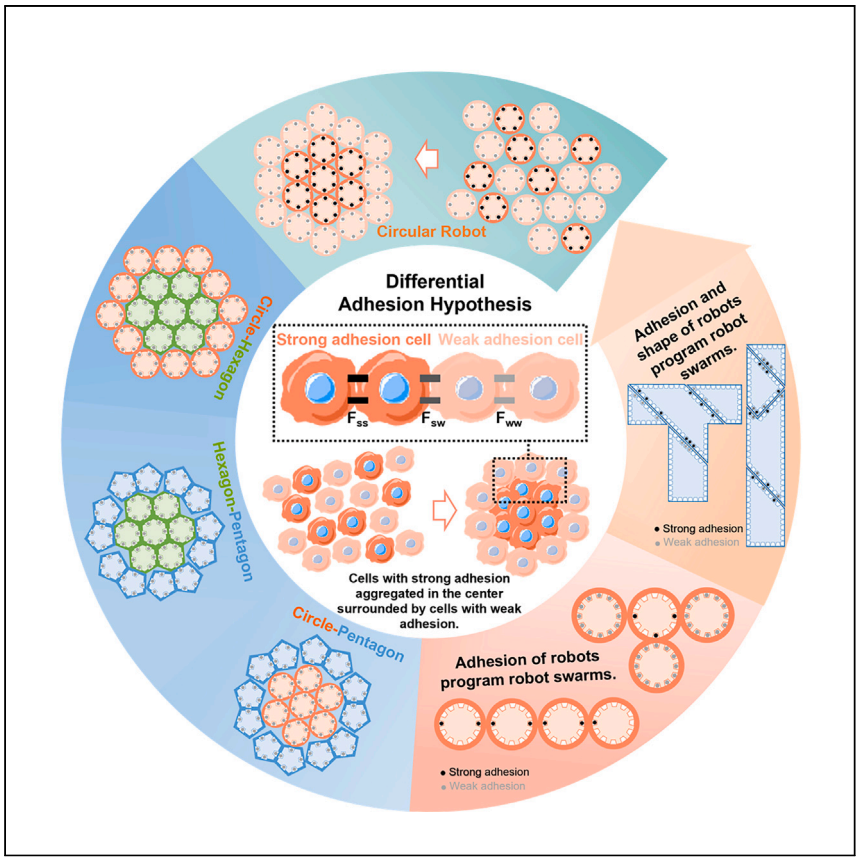

Physical intelligence is promising for developing robots with limited computational capabilities and in extreme conditions. Inspired by the physical principles of embryonic development, Pan et al. apply the differential adhesion hypothesis to program robot swarms, enabling them to form complex functional morphologies through physical interactions.

Mengyun Pan, Yongliang Yang, Xiaoyang Qin, ..., Lei Jiang, Tianming Zhao, Lianqing Liu

lqliu@sia.cn

Highlights

Physical principle of cell collectives is applied to program robot swarms

Swarms of sensor-less robots self-organize into functional morphologies

Differential adhesion hypothesis is studied in both robot swarms and cell collectives

Pan et al., Cell Reports Physical Science 5, 102122
August 21, 2024
https://doi.org/10.1016/j.xcrp.2024.102122

Cell Reports
Physical Science

CellPress
OPEN ACCESS

Article

Applying the intrinsic principle of cell collectives to program robot swarms

Mengyun Pan,[1,2] Yongliang Yang,[1] Xiaoyang Qin,[1,2] Guangyong Li,[3] Ning Xi,[4] Min Long,[5] Lei Jiang,[6] Tianming Zhao,[1] and Lianqing Liu[1,7,*]

SUMMARY

Many control algorithms for formation of robot swarms are often inspired by animal swarms. However, these algorithms require robots having sensing and computational capabilities and are not applicable to robot swarms working in extreme environments, such as at micro/nanoscale and in space. Here, we directly apply the differential adhesion hypothesis (DAH) of cell biology to the formation of robot swarms. Like cell collectives, swarms of sensor-less robots aggregate and sort in a self-organized manner. We quantitatively investigate the DAH principle in both swarms of cells and robots. We find that the sorting time is nonlinearly related to the levels of adhesion differences. This sheds light on the mechanisms of timing control in morphogenesis. Based on these findings, we program robot swarms to form functional morphologies by tuning their adhesion. This work advances swarm robotics in forming functional morphologies in a self-organized manner and enables us to investigate morphogenesis in cell collectives using robot swarms.

INTRODUCTION

Robot swarms are scalable, fault tolerant, flexible, and environmentally adaptable.[1,2] They thus have a wide range of potential applications, such as infrastructure inspection and search and rescue in disasters.[2] Large-scale robot swarms with complex hardware, however, are very expensive to construct and maintain.[2] The expected working environments for robot swarms, such as outer space, deep sea, and the human body, are harsh for mechanical and electrical elements of robots.[2–4] To deploy robot swarms in real-world applications, we need to design, fabricate, and control swarms of robots with minimal computation and perception (MCPR). Different MCPR systems have been proposed to emerge sophisticated global behaviors.[5–10] Cohesive granular robots rely on mechanical attraction between robots for aggregation and impurity transport.[5] Embedded locomotion active particles with mechanical interactions perform tasks.[6,7] Loosely coupled particle robots migrate by swelling and contracting.[8] Microbristle robots are designed using motion characteristics of robots for aggregation.[9]

A key challenge in swarm robotics is to develop a programmable self-organization approach to control MCPR swarms to form functional shapes.[1] Most control algorithms for robot swarms are inspired by self-organizing animal swarms, such as flocks of birds, schools of fish, ants, and bees.[1,3,11–13] These algorithms require highly intelligent robots and are derived by imitating the behaviors of animal swarms because of the capability gaps between animals and robots. However, this further hinders the application of robot swarms in the real world.

[1]State Key Laboratory of Robotics, Shenyang Institute of Automation, Chinese Academy of Sciences, Shenyang 110016, China

[2]University of the Chinese Academy of Sciences, Beijing 100049, China

[3]Department of Electrical and Computer Engineering, Swanson School of Engineering, University of Pittsburgh, Pittsburgh, PA, USA

[4]Advanced Technologies Institute, Department of Industrial and Manufacturing Systems Engineering, University of Hong Kong, Pokfulam, Hong Kong

[5]Department of Endocrinology, Southwest Hospital Affiliated to Army Medical University, Chongqing 400000, China

[6]China North Vehicle Research Institute, Beijing 100072, China

[7]Lead contact

*Correspondence: lqliu@sia.cn

https://doi.org/10.1016/j.xcrp.2024.102122

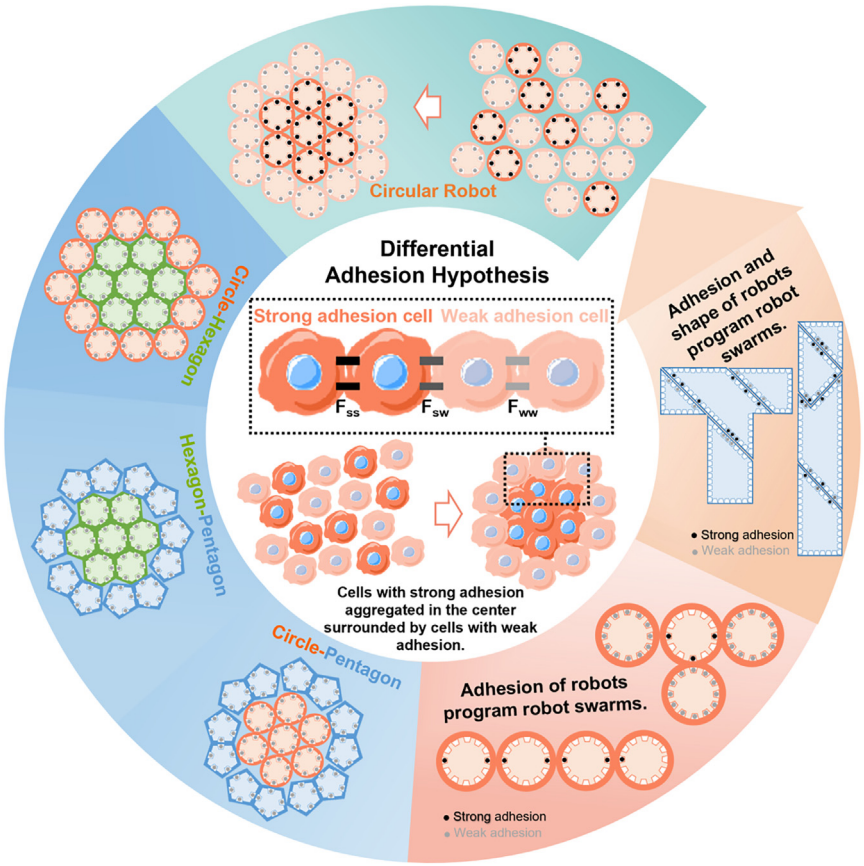

Figure 1. Applying the intrinsic principle of cell collectives to program robot swarms

The DAH proposes that cells with strong adhesion aggregate in the center, surrounded by cells with weak adhesion. Robot swarms can aggregate and sort for robots with different adhesion forces. For the same adhesion force, circle-hexagon, hexagon-pentagon, and circle-pentagon robot swarms can achieve robot aggregation and sorting. The functional morphologies can be achieved by programming the adhesion force and shape of robots. Black dots represent strong adhesion. Gray dots represent weak adhesion.

Cell collectives form sophisticated functional morphologies at the scale of tissues, organs, and individual animals through physical interactions controlled by biochemical signaling pathways and gene-regulatory networks.[14–19] Inspired by this, scientists in swarm robotics have long been dreaming of developing robot swarm systems that can evolve as embryos do.[20–22] Since the beginning of this century, biologists have advanced our understanding of the rules of mechanical forces in collective cell behaviors,[15,17] which offers opportunities for scientists in robotics. Inspired by the Turing pattern mechanism in developmental biology, Slavkov et al. created emergent morphologies in large robot swarms through self-organized local interactions.[23] The local interactions among robots were exchanging information via electrical computing instead of direct physical interactions. Recently, Li et al. designed a particle robot swarm system that could self-organize to accomplish tasks via physical interactions among neighboring robots.[8] Because the interaction rule of this system was much simpler than that of cell collectives, this system could not self-organize into complex pre-specified shapes or formations as cell collectives do. In cell biology, physical interactions, regulated by genes and molecules, play an important role in morphogenesis.[14–17] For example, a mixture of cells with different adhesion will sort into cellular aggregates with strong adhesion cells surrounded by weak adhesion cells (Figure 1). This phenomenon, the so-called differential adhesion hypothesis (DAH), has been investigated for almost a century in developmental

biology.[24–27] Under different conditions during embryo development, cell collectives can achieve different morphologies through the physical interaction-based DAH principle.[28–31] This physical intelligence in cell collectives has inspired algorithms for controlling robot swarms.[32,33] These algorithms, however, are not suitable for MCPRs because they apply artificial potential fields to robot swarms and require intensive on-board computation. Directly applying the DAH intrinsic principle might minimize the load on the computational intelligence of the robots.[34]

Here, we apply this physical intelligence in cell collectives to program MCPR swarms to form pre-defined functional morphologies (Figure 1). We find that robot swarms share the intrinsic principle of DAH in cell biology. The robots, without sensing and computing, aggregate and sort by directly changing the adhesion forces between robots or indirectly by changing the shapes of the robots. Using adhesion force and shapes of robots as variables, we program the robot swarm to form pre-defined functional morphologies in a self-organized manner. This physical intelligence enables us to quantitatively program robot swarms, which is critically important for developing MPCR swarms working in extreme conditions. Meanwhile, we find that the levels of adhesion differences nonlinearly affect the sorting time in both cell collectives and robot swarms. This mechanism of timing may be applied in robot swarm systems, also explaining timing control in embryo development. Combining robot swarms and cell collectives, a new research paradigm emerges to investigate and translate physical intelligence in developmental biology.

RESULTS

Robot swarms share the principle of DAH in cell biology

We directly applied the DAH principle of cell collectives to the formation of robot swarms. We first validated the DAH principle in cell collectives both in experiments and in simulations. Human gastric cancer cells (HGC-27) express less E-cadherin than human renal epithelial cells (HEK293) (Figure S2) and thus have weaker adhesion than HEK293 cells.[25–27] Starting from a mixture including the two types of cells in the experiments, HEK293 cells aggregated into a core, and HGC-27 cells enclosed the core within 15 h (Figure 2A). To exclude the effects induced by different cell types, we manipulated the expression of E-cadherin in HaCaT cells using small interfering RNA and repeated the cell sorting experiment. The cells with strong adhesion were surrounded by the cells with weak adhesion (Figures S1C and S1D). We further simulated the aggregation and sorting induced by differential adhesion among cells using CompuCell3D, a modeling software of virtual tissue.[35] The simulation results were similar to experimental results (Figure 2B). Since the main factor of the DAH principle is cellular adhesion rather than deformability of cells, we hypothesized that the DAH principle would also work in swarms of rigid robots. To test this hypothesis, we set up an MCPR swarm platform on a flat rectangular table (Figure 2C). An MCPR includes a changeable outer shell and a robotic base (Figure 2D). The robotic base of the MCPR includes a battery, a controller, and four vibrating needle legs. The MCPR has no capability of sensing and communication. During experiments, the trajectory of each MCPR is designed as an alternative sequence between straight lines and circles to avoid being blocked at the corners of the table. To mimic cellular adhesions, each MCPR was mounted with uniformly distributed magnets in its changeable outer shell with either strong or weak magnetic adhesion forces. After running for about 750 s, MCPRs with strong adhesion (orange MCPRs) aggregated in the center and were surrounded by MCPRs with weak adhesion (green MCPRs) (Figure 2E). These results demonstrated that the DAH principle is applicable to swarms of rigid robots.

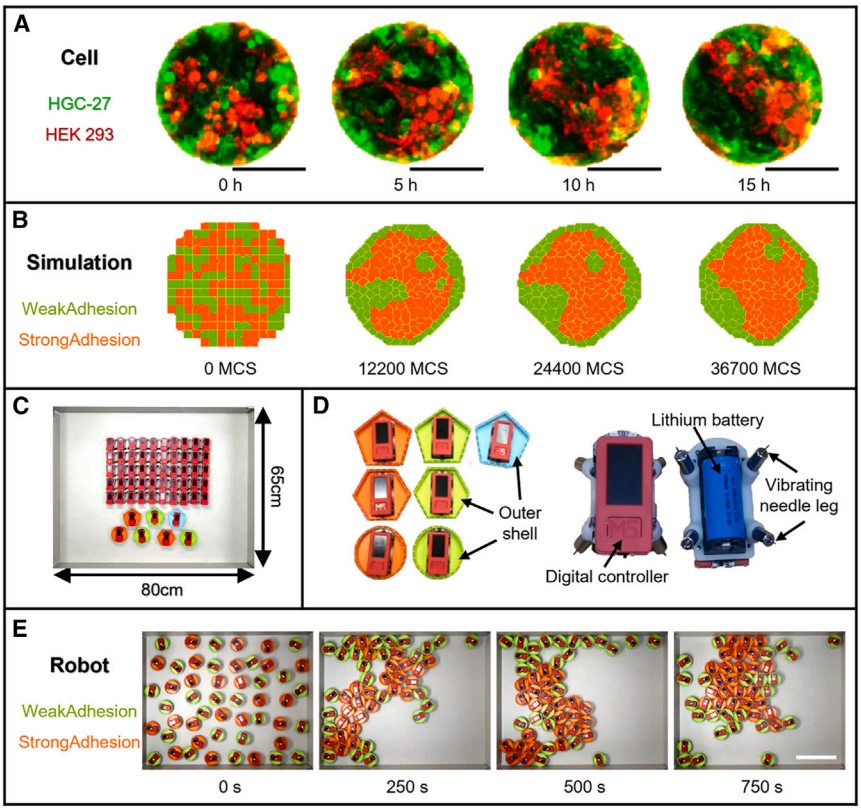

Figure 2. Robot swarms share the same principle of cell collectives

(A) A temporal sequence of the cell sorting experiment (from left to right). Red represents cells with strong adhesion, HEK293. Green represents cells with weak adhesion, HGC-27. Scale bars, 100 μm.

(B) A temporal sequence of simulation of cell sorting (from left to right).

(C) Two-dimensional experimental platform. The experimental platform is 80 cm × 65 cm.

(D) The design of robots. Each robot has a digital controller, a lithium battery, four vibrating needle legs, and an outer shell. The diameter and height of circular robot are approximately 63 mm and 37.5 mm, respectively. The magnets mounted on the outer shell of robots attract robots together.

(E) A temporal sequence of self-organized sorting of robot swarms (from left to right). Orange represents robots with strong adhesion. Green represents robots with weak adhesion. Scale bars, 20 cm.

Adhesion difference affects sorting of cell collectives and robot swarms

Although the DAH principle has been investigated intensively, how the level of adhesion difference affects aggregation and sorting of the agents is not yet clear. Here, we quantitatively investigated this and found that the sorting time peaks at the intermediate level of adhesion difference. We selected four cell types with different expression levels of E-cadherin, as indicated in fluorescence images. Thus, the cellular adhesion has four different levels: HGC-27 cells < HEK293 cells < MCF-7 (human breast cancer) cells < HaCaT (human epidermal) cells (Figure S2). Mixing HGC-27 cells, expressing E-cadherin at the lowest level, with the other three types of cells, we surprisingly found that the longest sorting time appeared at the intermediate level of adhesion difference with HGC-27 and MCF-7 cells (Figures 3A–3C). To exclude that this phenomenon is induced by biochemical effects rather than by the different levels of adhesion differences, we simulated the cell sorting processes with various levels of adhesion difference using Compucell3D. Consistent with the experimental results, the simulation results showed that the sorting time peaks at the intermediate level of adhesion difference (Figures 3D–3F). Will the robot swarms follow the same pattern? Under various levels of adhesion difference, swarms of circular robots all sorted (Figures 3G and 3H). Like

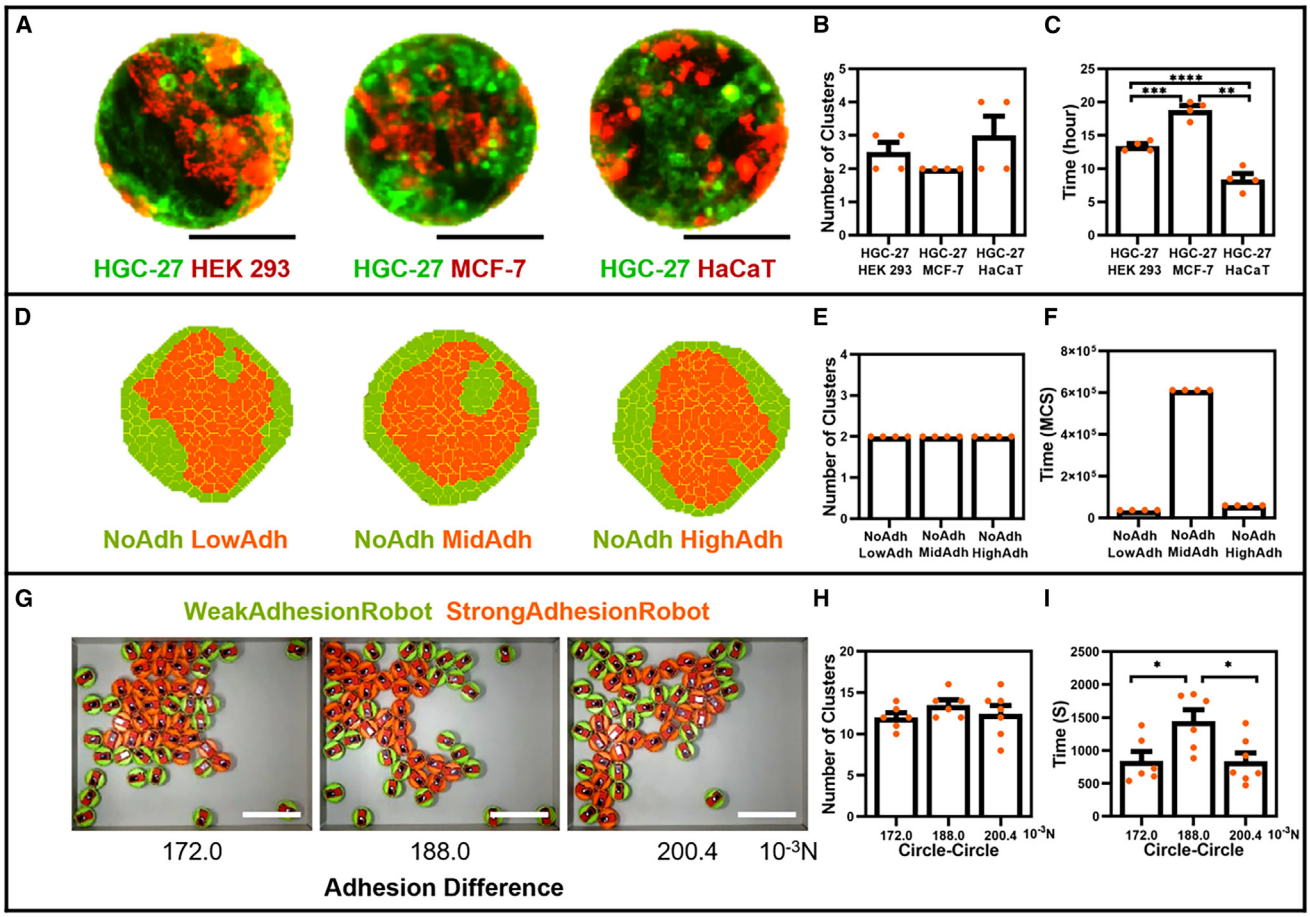

Figure 3. The level of adhesion difference affects aggregation and sorting of robot swarms and cell collectives

(A) The sorting results of two cell types with different adhesion. Scale bars, 100 μm.

(B) The number of clusters of cell sorting experiments.

(C) The sorting time of cell collectives with various levels of adhesion differences.

(D) The sorting results of two types of cells with different adhesion in simulation. NoAdh, LowAdh, MidAdh, and HighAdh represent the adhesion force from low to high respectively.

(E) The number of clusters of cell sorting in simulation.

(F) The sorting time of cell collectives with various levels of adhesion differences in simulation.

(G) The sorting results of circular robots with different adhesion forces. Orange represents robots with strong adhesion. Green represents robots with weak adhesion. The magnetic strength of the orange robots (strong adhesion) increases while keeping that of green robots (weak adhesion) the same. Adhesion difference represents magnetic adhesion force with different sizes on the orange robot and the green robot. Scale bars, 20 cm.

(H) The number of clusters of circular robots with different adhesion forces.

(I) The sorting time of circular robots with different adhesion forces.

Error bars represent SEM. Statistics: t test; *$p < 0.05$, **$p < 0.01$, ***$p < 0.001$, $p < 0.0001$. $n \geq 4$ independent experiments. See also Videos S1 and S2.

cell collectives, the longest period of robot sorting appeared at the intermediate level of adhesion difference (Figure 3I). In our experiments, along with the increase of adhesion forces among strong adhesion robots/cells, the adhesion forces among the strong adhesion robots/cells and the weak adhesion robots/cells also increased. However, we can decouple these two factors in simulations using CompuCell3D. We scanned these two adhesion forces and tested their effects on aggregation and sorting of cells in simulation experiments. The sorting time had two peaks by increasing adhesion forces among strong adhesion robots/cells (Figure S3B). The sorting time had one peak or two peaks by increasing the adhesion forces among the strong adhesion robots/cells and the weak adhesion robots/cells (Figure S3C). The

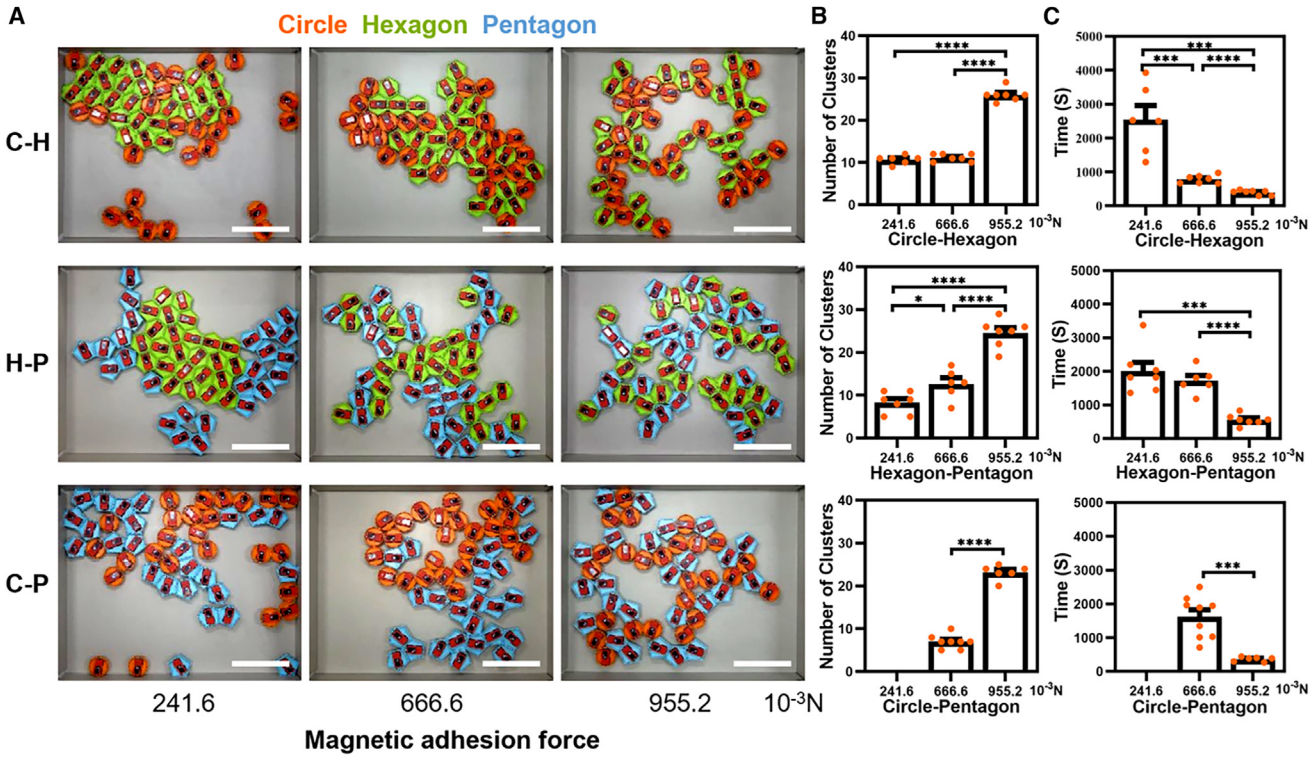

Figure 4. The shapes of robots affect aggregation and sorting of robot swarms

(A) The sorting results of robots with different shapes. Scale bars, 20 cm.

(B) The number of clusters of robots with different shapes.

(C) The sorting time of robots with different shapes.

Circular robots are orange. Hexagonal robots are green. Pentagonal robots are blue. C-H represents circle-hexagon. H-P represents hexagon-pentagon. C-P represents circle-pentagon. Magnetic adhesion force represents magnetic adhesion force with the same size on the robots. Error bars represent SEM. Statistics: t test; *$p < 0.05$, **$p < 0.01$, ***$p < 0.001$, ****$p < 0.0001$. $n \geq 4$ independent experiments. See also Video S3.

simulation results demonstrated that this simple phenomenon may have intricate mechanisms. The detailed information is provided in Figure S3. Although critically important for developmental biology,[36,37] timing has been paid far less attention in studies of the DAH principle due to the limits of experimental models. Our finding offers a potential mechanism for time controlling for morphogenesis during embryo development.

The shape of robots affects sorting of robots

In epithelium, the epithelial cells all appear to have different shapes and show epithelial polygons ranging from triangles to decagons, with a predominantly hexagonal cell pattern.[38] Deformable cells can form an integrated layer regardless of their shape, but rigid robots cannot. Hexagons tend to form a seamless layer, while pentagons and circles form a layer with gaps. In addition, the circular shells contact each other in a line, and the hexagonal and pentagonal shells contact each other at the interface area between robots. This geometrical difference affects adhesion forces between robots. Will the shape-induced adhesion difference aggregate and sort the robots? We designed hexagonal and pentagonal shells with the same magnetic strength. Consistent with the DAH principle, the hexagonal robots aggregated in the center in both the circle-hexagon robot swarm and hexagon-pentagon robot swarm (first column in Figure 4A). In the circle-pentagon robot swarm, the swarm cannot aggregate to form a pattern at the smallest adhesion force among

robots (third row in Figure 4). Increasing the adhesion force among robots, the robot swarms aggregated and sorted (third row in Figure 4A). When the adhesion force among robots is smaller than the driving force of the robots, the robots will disperse. A brief force model is provided in Figure S4. To explain the sorting induced by geometrical factors, we defined minimum swarms of three robots with the same shapes (Figure S5). The order of adhesion force of the minimum swarms is (1) hexagonal robots > pentagonal robots and (2) hexagonal robots > circular robots. The adhesion relationship between pentagonal robots and circular robots cannot be determined because the adhesion distribution of minimum swarms of pentagonal robots is not a stable triangle. A detailed description is provided in Figure S5. As we can see, the geometric shapes ultimately affect the adhesion force among robots, which affects the robot sorting. Last, we quantitatively characterized the effect of adhesion force on the sorting results. We found that the number of clusters in swarms increases and the time of sorting decreases with increasing magnetic strength of robots (Figures 4B and 4C). Increasing magnetic strength of robots increases all adhesion forces among robots, which facilitates aggregation of robots. A brief force model is provided in Figure S4.

The DAH programs robot swarms

The previous sections have demonstrated that both adhesion differences and shapes of robots affect the aggregation and sorting of robot swarms under the DAH principle. Based on DAH, we developed a programming method that uses adhesion differences among robots and shapes of robots as variables. By directly adjusting the adhesion differences among robots, circular robots self-organized into desired morphologies T and I (Figures 5A–5D). Via programming both adhesion differences among robots and shapes of robots, heterogeneous robots self-organized into desired functional morphologies as T and I (Figures 5E–5H). This method does not require computational intelligence because it only relies on emergent physical intelligence based on interactions among robots.[34] We used the shapes of a simple version of Tangram[39] as outer shells of robots and designed the adhesion distribution on these shells with no magnet, a weak magnet, and a strong magnet on each slot. The programming rule of adhesion distribution is described here. When two edges of outer shells match according to a pre-defined pattern, the adhesion force is larger than the driving force. Otherwise, the adhesion force between the edges is smaller than the driving force. Following this rule, we properly arranged the digital value for every slot on four robots with different shapes so that the robot swarm formed functional morphologies: a "T" shape and an "I" shape (Figures 5E–5H). The detailed rule is described in the supplemental information. This is the first realization of forming functional morphologies in self-organized systems via programming physical interactions among MCPRs. Using these functional morphologies, the robot swarm accomplished the task of completing the pattern "SIA," the logo of the Shenyang Institute of Automation (Figures 5I and 5J). The T-shaped robot swarm transported a cylinder to a defined position. The robots were then self-organized into an "I" shape and positioned under the dot to form an "i."

DISCUSSION

In this study, we demonstrated that robot swarms share the same DAH principle with cell collectives through both simulation and experiments. We applied the intrinsic principle of DAH to program robot swarms toward forming pre-defined functional morphologies. We then quantitatively investigated the DAH principle in cell and robot swarms, respectively. We found that the level of adhesion differences affected

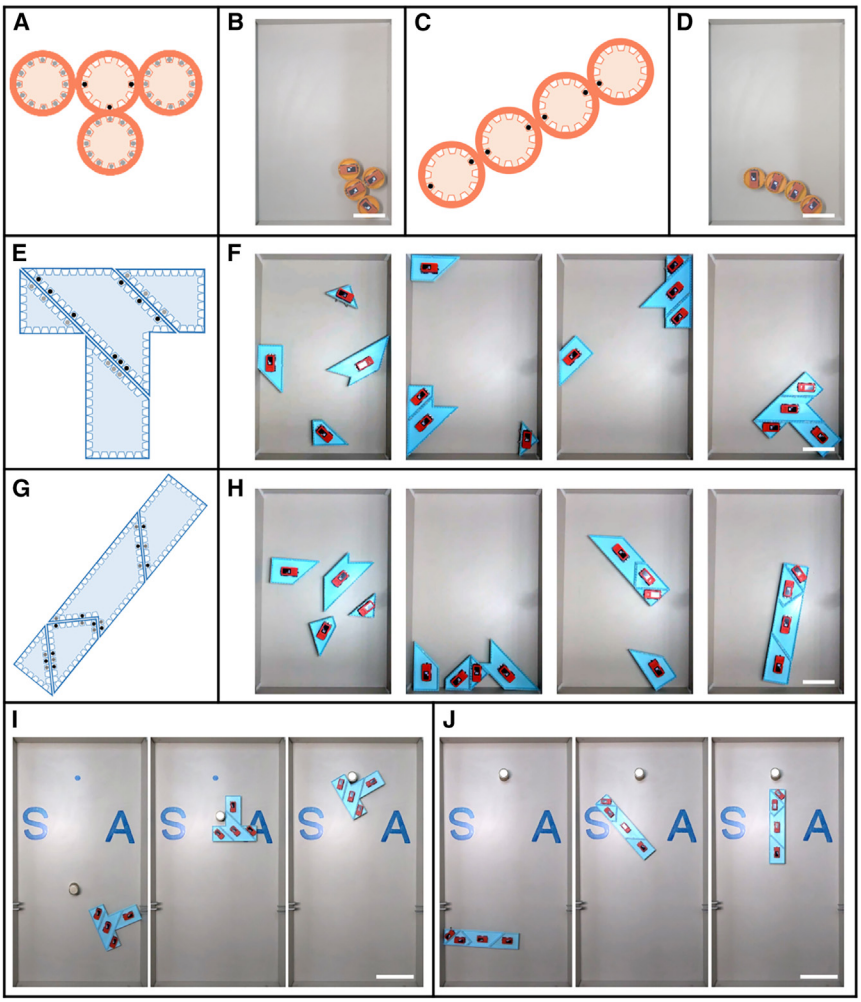

Figure 5. Adhesion and shape of robots program robot swarms

(A) The magnet positions of circular robots forming a "T" shape.
(B) The circular robots formed a "T" shape. Scale bar, 10 cm.
(C) The magnet positions of circular robots forming an "I" shape.
(D) The circular robots formed an "I" shape. Scale bar, 10 cm.
(E) The magnet positions of "T" robots.
(F) Self-assembly process of "T" robots (from left to right). Scale bars, 10 cm.
(G) The magnet positions of "I" robots.
(H) Self-assembly process of "I" robots (from left to right). Scale bars, 10 cm.
(I) A sequence of images presenting the process (beginning from the left) of the "T" robots transporting a column. Scale bars, 20 cm.
(J) A temporal sequence of the "I" robots completing the logo of the Shenyang Institute of Automation (from left to right). The experimental platform is 120 cm × 65 cm. Black dots represent strong adhesion. Gray dots represent weak adhesion. See also Video S4. Scale bars, 20 cm.

the timing of sorting in swarms of robots and cells. Instead of using sensing and computing, we directly programmed heterogeneous robots through adhesion differences among robots and shapes of robots. The results presented in this paper will advance swarm robotics from simply imitating behaviors of natural swarms to quantitatively applying intrinsic principles to program robot swarms.

Scientists in swarm robotics have benefitted significantly from scientists investigating natural swarms. But scientists studying natural swarms seldom benefit from the advances of swarm robotics.[2] Robot swarms have unique advantages for investigating the

behaviors of cell collectives. Compared to *in vitro* cell experiments, robot swarms are easier to manipulate and observe. Meanwhile, robot swarms can decouple the biophysical subsystem from the biochemical subsystem in cell biology, as biochemistry decouples the biochemical subsystem from the biophysical subsystem in cell biology. Although the DAH principle has been intensively studied in the past century, some of its physical features have not been quantitatively investigated because intercellular adhesion is difficult to manipulate due to its complicated molecular mechanisms.[27] In robot swarms, however, we can easily manipulate the adhesion among robots. Using both robot swarms and cell collectives, we found that the sorting time of both types of swarms is related to the levels of adhesion differences (Figure 3). It has been reported that cells in embryos bud out to form tree structures with uneven reduction of E-cadherin expression from the center to the boundary of the tissue.[30] Based on our findings, we hypothesize that differences in the gradients of E-cadherin expression may be a means to time the budding process. The relationship between physical interactions and gene-regulatory networks has been a key question in developmental biology.[17] Slavkov et al. have demonstrated that robot swarms share gene-regulatory networks with cell collectives,[23] and we demonstrated that the two also share physical principles during morphogenesis. Integrating these two directions, we may develop a robot swarm system for cell biologists to investigate the interplay of gene-regulatory networks and physical interactions.

Since the local interactions among robots relate to the global morphology in an implicit manner,[3,11] it is difficult to define a programming rule for local interactions toward global patterns, especially for physical interactions.[22] This is a key challenge of morphological engineering in self-organized systems.[1,22] While there have been some advances in algorithms for physical interaction, especially in the field of modular robotics,[40,41] these algorithms still require heavy communication between robots. Here, we defined a simple rule of physical interaction among robots. This rule bridges the global functional morphologies and features of individual robots. It thus is a good example of emergent physical intelligence in robot swarms.[34] The functional morphologies determine whether the local interaction is stable, and the local interaction is controlled by the robot adhesion forces; that is, the magnet distribution or shape of a single robot. Given the functional morphologies, the positions of magnets on the outer shell are determined by trial and error. In self-organized systems, it is still not clear how to find low-level rules that can result in specific global outcomes.[11,42] Werfel et al. proposed an example where a termite-inspired robot system automatically generates low-level rules to build user-specified structures.[11] Because only three robots existed in their swarm system, their work might not function for large robot swarms. We believe that the machine learning and data-driven research paradigm might offer solutions to the problem of large robot swarms.[43] Slavkov et al. pointed out that forming functional shapes requires a more detailed theoretical understanding of governing principles.[23] By quantitatively investigating the DAH principle in cell and robot swarms, respectively, we were able to program heterogeneous robots with functional morphologies. Applying cellular mechanisms of both physical interactions and gene-regulatory networks to robot swarms, we may realize hierarchical control for them to accomplish sophisticated tasks in complex environments.[2,44] This will push the robot swarms further toward embodied systems.[45,46]

EXPERIMENTAL PROCEDURES

Resource availability

Lead contact

Requests for further information, resources, and reagents should be directed to and will be fulfilled by the lead contact, Lianqing Liu (lqliu@sia.cn).

Materials availability

This study did not generate new unique materials.

Data and code availability

The data underlying this study are available in the article and supplemental information or from the lead contact upon request.

Cell lines and culture

The HEK293 immortalized cell line was purchased from the National Collection of Authenticated Cell Cultures (Shanghai, China). The HGC-27 gastric cancer cell line was purchased from the Institute of Biochemistry and Cell Biology, Chinese Academy of Sciences (Shanghai, China). DMEM (DearyTech, DT-12800) medium was supplemented with 10% fetal bovine serum (FBS) and 1% penicillin-streptomycin to make DMEM complete medium. HEK293, MCF-7, HaCaT, and HGC-27 cells were cultured in DMEM complete medium in an incubator at 37°C and 5% CO_2. For passaging, after rinsing with PBS (DearyTech, DT-20012), all cells were treated with 0.25% trypsin-EDTA to detach from the dish.

Fabrication of circular microstructures

Microstructures were 3D printed using a commercially available two-photon polymerization system (Photonic Professional GT2, Nanoscribe, Germany) with a 25× objective (numerical aperture = 0.8) and IP-S resin on an indium tin oxide-coated glass substrate. Following fabrication, the microstructures were developed with propylene glycol methyl ether acetate solution for 20 min and isopropanol for 30 s to remove the remaining resin. After development, the microstructures were cured under UV light to solidify unprinted IP-S resin.

Cell sorting and live imaging

The cells were stained separately with 1,1′-dioctadecyl-3,3,3′,3′-tetramethylindocarbocyanine perchlorate (C1991S, Beyotime) or 3,3′-dioctadecyloxacarbocyanine perchlorate (C1993S, Beyotime) for 20 min at 37°C. Cells were washed extensively with medium after staining. The dye-stained cells were mixed at ratios of 1:1 (HEK293:HGC-27 = 1:1, MCF-7:HGC-27 = 1:1, and HaCaT:HGC-27 = 1:1). The mixture of cells was added to a dish with microstructures at 1.8 million cells/mL. After 5 h of static culture, the medium was changed to remove excessive cells. Fluorescence images of the sorting process were recorded using a spinning disk confocal microscope (Crest Optics X-Light V3, Nikon) every 15 min for 30 h in an onstage cell culture chamber (37°C and 5% CO_2).

Image acquisition and analysis

All images acquired on the Nikon spinning disk confocal microscope were denoised using the Nikon NIS-Elements software. ImageJ software (https://imagej.nih.gov/ij/) was used to analyze the E-cadherin fluorescence intensity of cells. The number of independent experiments and the statistical test employed are indicated in the respective figure legends. A p value less than 0.05 was statistically significant.

Robot design

Each robot contains a lithium battery (M5Stack), development board (StickC PLUS: M5Stack), programmable robot base (BugC: M5Stack), outer shell, and magnets. M5StickC PLUS is a portable open-source Internet of Things development board. It is equiped with an ESP32-PICO-D4 microcontroller with Wi-Fi. M5StickC PLUS can be programmed using C language on the Arduino integrated development environment. BugC is a programmable robot base with four direct current motors and

their drivers, two red-green-blue light-emitting diode lights, a battery holder, and a switch. BugC is equiped with an STM32F030F4 microcontroller, which can control all motors using the I2C protocol (0 × 38) through the M5StickC controller. The outer shells are 3D printed in polylactic acid plastic. The pentagonal outer shells and hexagonal outer shells are external polygons of circular outer shells. The neodymium iron boron magnets with nickel plating are mounted on the outer shells to generate adhesion forces of robots. Several magnets with different sizes were used to adjust the adhesion forces.

Robot motion

The speed of each robot was set at a constant. The trajectory of each robot is designed as an alternative between straight lines and circles to avoid being blocked at the corners of the table. Due to the variation of motors, the trajectories of robots have a large deviation.

Sizes of magnets and their positions on the outer shells

All magnets are circles, with specific sizes of 3 mm × 1 mm, 4 mm × 1 mm, 4 mm × 1.5 mm, 5 mm × 1.5 mm, and 6 mm × 1.5 mm (diameter × thickness). The sizes of magnets used in Figure 3 were 3 mm × 1 mm:4 mm × 1.5 mm, 3 mm × 1 mm:5 mm × 1.5 mm, and 3 mm × 1 mm:6 mm × 1.5 mm. Twelve magnets are evenly arranged on the circular outer shell. The green robots had weak adhesion force, and the size of the magnets was 3 mm × 1 mm. The orange robots had strong adhesion force, and the sizes of the magnets were 4 mm × 1.5 mm, 5 mm × 1.5 mm, and 6 mm × 1.5 mm.

The sizes of magnets used in Figure 4 were 4 mm × 1 mm, 5 mm × 1.5 mm, and 6 mm × 1.5 mm. Twelve magnets are evenly arranged on the outer shell. The circular robots were orange, the hexagonal robots were green, and the pentagonal robots were blue.

The sizes of magnets used in Figure 5 were 5 mm × 1 mm and 6 mm × 1.5 mm. The positions of the magnets are shown in Figure 5. The gray one was 5 mm × 1 mm, and the black one was 6 mm × 1.5 mm.

Functional morphologies accomplish tasks

The functional morphology "T" or "I" was formed with four robots. Each robot was connected to the MQTTX cloud platform built on the computer through Wi-Fi. The motion of the functional morphology as a whole required all robots to work together. Thus, we designed four control commands, W, S, A, and D, to control the motion of the functional morphology. W was for the forward command, S was for the backward command, A was for the counterclockwise rotation command, and D was for the clockwise rotation command.

SUPPLEMENTAL INFORMATION

Supplemental information can be found online at https://doi.org/10.1016/j.xcrp.2024.102122.

ACKNOWLEDGMENTS

This research was supported by the National Natural Science Foundation of China (grants 61925307 and 62273338) and in part by the Open Fund Project of the Collective Intelligence and Collaboration Laboratory (grant numbers QXZ23013401).

We thank Dr. Lingli Yu at Central South University and Dr. Jianguo Zhao at Colorado State University for discussion during research.

AUTHOR CONTRIBUTIONS

Y.Y. and M.P. conceived the idea. Y.Y. and L.L. supervised the project. M.P., Y.Y., N.X., and L.L. designed the experiments. M.P., X.Q., T.Z., and L.J. designed the robot swarm system. M.L. helped design the experiments with cells. T.Z. and L.J. helped design the experiments with robots. M.P. conducted the experiments and wrote the first draft of this paper. G.L., L.J., T.Z., M.L., Y.Y., and L.L. commented on, revised, and edited the paper.

DECLARATION OF INTERESTS

The authors declare no competing interests.

Received: March 13, 2024
Revised: June 7, 2024
Accepted: July 5, 2024
Published: July 26, 2024

REFERENCES

1. Dorigo, M., Theraulaz, G., and Trianni, V. (2020). Reflections on the future of swarm robotics. Sci. Robot. *5*, eabe4385.
2. Dorigo, M., Theraulaz, G., and Trianni, V. (2021). Swarm Robotics: Past, Present, and Future [Point of View]. Proc. IEEE *109*, 1152–1165.
3. Berlinger, F., Gauci, M., and Nagpal, R. (2021). Implicit coordination for 3D underwater collective behaviors in a fish-inspired robot swarm. Sci. Robot. *6*, eabd8668.
4. Sitti, M., and Wiersma, D.S. (2020). Pros and Cons: Magnetic versus Optical Microrobots. Adv. Mater. *32*, 1906766–1906810/ghpj7v.
5. Li, S., Dutta, B., Cannon, S., Daymude, J.J., Avinery, R., Aydin, E., Richa, A.W., Goldman, D.I., and Randall, D. (2021). Programming active cohesive granular matter with mechanically induced phase changes. Sci. Adv. *7*, eabe8494.
6. Boudet, J.F., Lintuvuori, J., Lacouture, C., Barois, T., Deblais, A., Xie, K., Cassagnere, S., Tregon, B., Brückner, D.B., Baret, J.C., and Kellay, H. (2021). From collections of independent, mindless robots to flexible, mobile, and directional superstructures. Sci. Robot. *6*, eabd0272.
7. Savoie, W., Berrueta, T.A., Jackson, Z., Pervan, A., Warkentin, R., Li, S., Murphey, T.D., Wiesenfeld, K., and Goldman, D.I. (2019). A robot made of robots: Emergent transport and control of a smarticle ensemble. Sci. Robot. *4*, eaax4316.
8. Li, S., Batra, R., Brown, D., Chang, H.-D., Ranganathan, N., Hoberman, C., Rus, D., and Lipson, H. (2019). Particle robotics based on statistical mechanics of loosely coupled components. Nature *567*, 361–365.
9. Hao, Z., Mayya, S., Notomista, G., Hutchinson, S., Egerstedt, M., and Ansari, A. (2023). Controlling Collision-Induced Aggregations in a Swarm of Micro Bristle Robots. IEEE Trans. Robot. *39*, 590–604.
10. Qin, X., Yang, Y., Pan, M., Cui, L., and Liu, L. (2023). Morphobot: A Platform for Morphogenesis in Robot Swarm. IEEE Rob. Autom. Lett. *8*, 7440–7447. https://doi.org/10.1109/LRA.2023.3320021.
11. Werfel, J., Petersen, K., and Nagpal, R. (2014). Designing Collective Behavior in a Termite-Inspired Robot Construction Team. Science *343*, 754–758.
12. Kernbach, S., Thenius, R., Kernbach, O., and Schmickl, T. (2009). Re-embodiment of Honeybee Aggregation Behavior in an Artificial Micro-Robotic System. Adapt. Behav. *17*, 237–259.
13. Duan, H., Huo, M., and Fan, Y. (2023). From animal collective behaviors to swarm robotic cooperation. Natl. Sci. Rev. *10*, nwad040. https://doi.org/10.1093/nsr/nwad040.
14. Hogan, B.L.M. (1999). Morphogenesis. Cell *96*, 225–233.
15. Heisenberg, C.-P., and Bellaïche, Y. (2013). Forces in Tissue Morphogenesis and Patterning. Cell *153*, 948–962.
16. Ladoux, B., and Mège, R.-M. (2017). Mechanobiology of collective cell behaviours. Nat. Rev. Mol. Cell Biol. *18*, 743–757. https://doi.org/10.1038/nrm.2017.98.
17. Dance, A. (2021). The secret forces that squeeze and pull life into shape. Nature *589*, 186–188.
18. Collinet, C., and Lecuit, T. (2021). Programmed and self-organized flow of information during morphogenesis. Nat. Rev. Mol. Cell Biol. *22*, 245–265.
19. Adler, F.R., Anderson, A.R.A., Bhushan, A., Bogdan, P., Bravo-Cordero, J.J., Brock, A., Chen, Y., Cukierman, E., DelGiorno, K.E., Denis, G.V., et al. (2023). Modeling collective cell behavior in cancer: Perspectives from an interdisciplinary conversation. Cell Syst. *14*, 252–257. https://doi.org/10.1016/j.cels.2023.03.002.
20. Fukuda, T., and Kawauchi, Y. (1990). Cellular robotic system (CEBOT) as one of the realization of self-organizing intelligent universal manipulator. In Proceedings 1990 IEEE International Conference on Robotics and Automation, pp. 662–667. https://doi.org/10.1109/ROBOT.1990.126059.
21. Rubenstein, M., Sai, Y., Chuong, C.-M., and Shen, W.-M. (2009). Regenerative patterning in Swarm Robots: mutual benefits of research in robotics and stem cell biology. Int. J. Dev. Biol. *53*, 869–881.
22. R. Doursat, H. Sayama, and O. Michel, eds. (2012). Morphogenetic Engineering: Toward Programmable Complex Systems (Springer Berlin Heidelberg). https://doi.org/10.1007/978-3-642-33902-8.
23. Slavkov, I., Carrillo-Zapata, D., Carranza, N., Diego, X., Jansson, F., Kaandorp, J., Hauert, S., and Sharpe, J. (2018). Morphogenesis in robot swarms. Sci. Robot. *3*, eaau9178.
24. Steinberg, M.S. (1963). Reconstruction of tissues by dissociated cells. Some morphogenetic tissue movements and the sorting out of embryonic cells may have a common explanation. Science, New Series *141*, 401–408.
25. Duguay, D., Foty, R.A., and Steinberg, M.S. (2003). Cadherin-mediated cell adhesion and tissue segregation: qualitative and quantitative determinants. Dev. Biol. *253*, 309–323.
26. Foty, R.A., and Steinberg, M.S. (2005). The differential adhesion hypothesis: a direct evaluation. Dev. Biol. *278*, 255–263.
27. Borghi, N., and James Nelson, W. (2009). Intercellular Adhesion in Morphogenesis. In Current Topics in Developmental Biology

(Elsevier), pp. 1–32. https://doi.org/10.1016/S0070-2153(09)89001-7.

28. Chanson, L., Brownfield, D., Garbe, J.C., Kuhn, I., Stampfer, M.R., Bissell, M.J., and LaBarge, M.A. (2011). Self-organization is a dynamic and lineage-intrinsic property of mammary epithelial cells. Proc. Natl. Acad. Sci. USA *108*, 3264–3269.

29. Cerchiari, A.E., Garbe, J.C., Jee, N.Y., Todhunter, M.E., Broaders, K.E., Peehl, D.M., Desai, T.A., LaBarge, M.A., Thomson, M., and Gartner, Z.J. (2015). A strategy for tissue self-organization that is robust to cellular heterogeneity and plasticity. Proc. Natl. Acad. Sci. USA *112*, 2287–2292.

30. Wang, S., Matsumoto, K., Lish, S.R., Cartagena-Rivera, A.X., and Yamada, K.M. (2021). Budding epithelial morphogenesis driven by cell-matrix versus cell-cell adhesion. Cell *184*, 3702–3716.e30. https://doi.org/10.1016/j.cell.2021.05.015.

31. Toda, S., Blauch, L.R., Tang, S.K.Y., Morsut, L., and Lim, W.A. (2018). Programming self-organizing multicellular structures with synthetic cell-cell signaling. Science *361*, 156–162.

32. Kumar, M., Garg, D.P., and Kumar, V. (2010). Segregation of Heterogeneous Units in a Swarm of Robotic Agents. IEEE Trans. Automat. Control *55*, 743–748.

33. Santos, V.G., Pires, A.G., Alitappeh, R.J., Rezeck, P.A.F., Pimenta, L.C.A., Macharet, D.G., and Chaimowicz, L. (2020). Spatial segregative behaviors in robotic swarms using differential potentials. Swarm Intell. *14*, 259–284.

34. Sitti, M. (2021). Physical intelligence as a new paradigm. Extreme Mech. Lett. *46*, 101340. https://doi.org/10.1016/j.eml.2021.101340.

35. Swat, M.H., Thomas, G.L., Belmonte, J.M., Shirinifard, A., Hmeljak, D., and Glazier, J.A. (2012). Chapter 13 - Multi-Scale Modeling of Tissues Using CompuCell3D. In Methods in Cell Biology Computational Methods in Cell Biology, A.R. Asthagiri and A.P. Arkin, eds. (Academic Press), pp. 325–366. https://doi.org/10.1016/B978-0-12-388403-9.00013-8.

36. Kiessling, A.A. (2010). Timing is everything in the human embryo. Nat. Biotechnol. *28*, 1025–1026. https://doi.org/10.1038/nbt1010-1025.

37. Rankin, S.A., McCracken, K.W., Luedeke, D.M., Han, L., Wells, J.M., Shannon, J.M., and Zorn, A.M. (2018). Timing is everything: Reiterative Wnt, BMP and RA signaling regulate developmental competence during endoderm organogenesis. Dev. Biol. *434*, 121–132. https://doi.org/10.1016/j.ydbio.2017.11.018.

38. Gibson, M.C., Patel, A.B., Nagpal, R., and Perrimon, N. (2006). The emergence of geometric order in proliferating metazoan epithelia. Nature *442*, 1038–1041.

39. Wang, F.T., and Hsiung, C.-C. (1942). A Theorem on the Tangram. Am. Math. Mon. *49*, 596–599. https://doi.org/10.2307/2303340.

40. Ahmadzadeh, H., Masehian, E., and Asadpour, M. (2016). Modular Robotic Systems: Characteristics and Applications. J. Intell. Rob. Syst. *81*, 317–357. https://doi.org/10.1007/s10846-015-0237-8.

41. Yim, M., Shen, W., Salemi, B., Rus, D., Moll, M., Lipson, H., Klavins, E., and Chirikjian, G.S. (2007). Modular Self-Reconfigurable Robot Systems [Grand Challenges of Robotics]. IEEE Robot. Autom. Mag. *14*, 43–52. https://doi.org/10.1109/MRA.2007.339623.

42. Doursat, R., Sayama, H., and Michel, O. (2012). Morphogenetic Engineering: Reconciling Self-Organization and Architecture. In Morphogenetic Engineering: Toward Programmable Complex Systems, R. Doursat, H. Sayama, and O. Michel, eds. (Springer), pp. 1–24. https://doi.org/10.1007/978-3-642-33902-8_1.

43. D'Souza, R.M., Di Bernardo, M., and Liu, Y.-Y. (2023). Controlling complex networks with complex nodes. Nat. Rev. Phys. *5*, 250–262. https://doi.org/10.1038/s42254-023-00566-3.

44. Mathews, N., Christensen, A.L., O'Grady, R., Mondada, F., and Dorigo, M. (2017). Mergeable nervous systems for robots. Nat. Commun. *8*, 439. https://doi.org/10.1038/s41467-017-00109-2.

45. Pfeifer, R., Lungarella, M., and Iida, F. (2007). Self-Organization, Embodiment, and Biologically Inspired Robotics. Science *318*, 1088–1093. https://doi.org/10.1126/science.1145803.

46. Miriyev, A., and Kovač, M. (2020). Skills for physical artificial intelligence. Nat. Mach. Intell. *2*, 658–660. https://doi.org/10.1038/s42256-020-00258-y.